WARSAW UNIVERSITY OF TECHNOLOGY Index 351733
FACULTY OF CIVIL ENGINEERING
COMMITTEE FOR CIVIL AND WATER ENGINEERING
POLISH ACADEMY OF SCIENCES ISSN 1230-2945

DOI: 10.24425/ace.2025.155108
ARCHIVES OF CIVIL ENGINEERING
Vol. LXXI ISSUE 3 2025
pp. 415–430

Research paper

Analysis of the critical stress intensity factor of concrete with gravel and dolomite aggregates tested by different methods

Amanda Akram[1], Marta Słowik[2], Marta Kosior-Kazberuk[3], Julita Krassowska[4]

Abstract: The cracking resistance of concrete is of paramount importance in the context of structural integrity and stability. Therefore, analysing fracture propagation in concrete is essential to evaluate resistance to crack propagation. The critical stress intensity factor K_{Ic} is one of the most often used fracture parameters when analysing fracture processes in concrete members. The critical stress intensity factor can be evaluated through standard laboratory tests described in RILEM recommendations. Digital image correlation (DIC) is a new measurement technique that provides the possibility of determining K_{Ic} in an alternative way. However, both measurement methods are subjected to certain challenges that may affect the results obtained. The question arises of whether the measurements by the standard RILEM method and by the method based on DIC give comparable results of concrete fracture parameters. The experimental investigation presented in the research paper deals with comparing test results of K_{Ic}, which were measured by two testing methods. To determine the critical stress intensity factor of concrete, the standard method based on the three-point bend test was applied as the basic testing method, and the ARAMIS 2D system based on DIC was used as a second testing approach. Moreover, aspects such as the influence of the type of aggregate on K_{Ic} and whether the type of aggregate would make a difference when assessing the impact of the test method on the results of K_{Ic} were analysed.

Keywords: concrete, critical stress intensity factor, digital image correlation, fracture parameters

[1]MSc., Eng., Lublin University of Technology, Faculty of Civil Engineering and Architecture, Nadbystrzycka 40, 20-618 Lublin, Poland, e-mail: a.akram@pollub.pl, ORCID: 0000-0001-5619-2927
[2]DSc., PhD., Eng., Lublin University of Technology, Faculty of Civil Engineering and Architecture, Nadbystrzycka 40, 20-618 Lublin, Poland, e-mail: m.slowik@pollub.pl, ORCID: 0000-0001-9627-3625
[3]DSc., PhD., Eng., Białystok University of Technology, Faculty of Civil Engineering and Environmental Sciences, Wiejska 45A, 15-351 Bialystok, Poland, e-mail: m.kosior@pb.edu.pl, ORCID: 0000-0001-8171-2242
[4]PhD., Eng., Białystok University of Technology, Faculty of Civil Engineering and Environmental Sciences, Wiejska 45A, 15-351 Bialystok, Poland, e-mail: j.krassowska@pb.edu.pl, ORCID: 0000-0001-9209-1285

1. Introduction

Concrete is one of the most widely used construction materials due to its strength, durability and versatility. The properties of concrete are influenced by various factors [1, 2], with the aggregate playing a crucial role in determining its performance under different loading conditions [3–6]. While compressive strength is a fundamental parameter for assessing the load-bearing capacity of concrete, it does not provide a comprehensive understanding of the material's behaviour. Particularly, the cracking resistance of concrete is of paramount importance in the context of structural integrity and stability. Therefore, analysing fracture processes in concrete is essential to evaluate resistance to crack propagation.

Investigations on the cracking resistance of concrete from a fracture mechanics point of view rely on determining various fracture parameters, such as the fracture energy, the critical crack size and the critical stress intensity factor (K_{Ic}). These parameters offer insights into the fracture behaviour of concrete and its ability to resist cracking under varying conditions. Research results presented in the literature indicate that the water-cement ratio [7, 8], the use of admixtures [9–12] and the aggregate properties such as the petrographic composition and geometry affect concrete properties, including the fracture parameters of concrete [13–15].

K_{Ic} is one of the most often used fracture parameters when analysing fracture processes in concrete members. Several experimental investigations have been carried out to measure the critical stress intensity factor and to analyse the impact of the aggregate type and the maximum aggregate size on K_{Ic} [16, 17]. However, it is difficult to obtain converged results due to the fact that experiments have not been conducted in a comprehensive manner. The critical stress intensity factor is evaluated through laboratory tests and finite element analysis [18, 19]. The standard testing method is based on the three-point bend test and is described in RILEM recommendations [20]. Digital image correlation (DIC) is a new measurement technique [21–24] that provides the possibility of determining K_{Ic} in an alternative way. However, both measurement methods are subjected to certain challenges that may affect the results obtained.

The standard RILEM approach is widely recognised as a method of gathering laboratory data in a three-point bend test, necessary for determining the fracture parameters of concrete. It requires a traditional testing setup with a hydraulic press for performing a bend test. However, the correct installation of the gauge at the initial crack is a crucial factor, as human error may occur. Furthermore, the method is also limited in its ability to capture detailed strain and deformation data.

The ARAMIS 2D system (based on DIC technology) enables non-contact measurement of surface strains and displacements during the three-point bend tests. It provides high-resolution, detailed strain and deformation data for the tested specimen, allowing for a more comprehensive analysis, including the investigation of crack development. However, the accuracy of the collected data depends on the initial parameters entered into the program prior to the start of the test, such as the frequency of image shooting. If the frequency is too low, there may not be enough information obtained from the test to calculate the critical stress intensity factor properly. The quality of the surface component, which is built by the ARAMIS 2D system based on the first reference image prior to the start of the laboratory test, is another aspect that should be considered in order to obtain the correct final results. A flawed surface

component will not allow to gather data for further fracture parameters calculations. Data processing and analysis also require specialised software and computational resources. On the other hand, not all laboratories have access to new measurement systems like ARAMIS.

The question arises of whether the measurements by the standard RILEM method and by the method based on DIC give comparable results of concrete fracture parameters, such as the critical stress intensity factor. The experimental investigation presented in the research paper deals with comparing test results of K_{Ic}, which were measured by two testing methods. To determine the critical stress intensity factor of concrete, the standard method described in RILEM recommendations [20] was applied as the basic testing method, and the ARAMIS 2D system was used as a second testing approach. Moreover, aspects such as the influence of the type of aggregate on K_{Ic} and whether the type of aggregate would make a difference when assessing the impact of the test method on the results of K_{Ic} were analysed.

2. Measurement methods

2.1. The standard RILEM method

The RILEM guidelines [20] address the determination of the critical stress intensity factor through the three-point bend tests conducted on a notched beam. The critical stress intensity factor is defined as the stress intensity factor calculated at the critical effective crack tip, utilising the measured maximum load. For the three-point bend test, the closed-loop hydraulic press can be used. Cyclic loading is applied to a beam specimen, and the crack mouth opening displacement (CMOD) is obtained as the feedback signal for the tested specimen using the clip gauge axial extensometers. The CMOD and the applied load (P) are recorded continuously during the test. The loading setup for the three-point bend test is shown in Fig. 1.

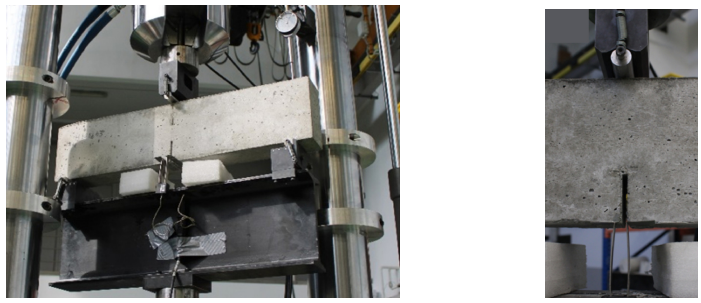

(a) (b)

Fig. 1. The general loading arrangement for the three-point bend test in accordance with RILEM [20] (a) and a close-up of the initial notch (b)

2.2. The DIC-based method

During the three-point bend test, a high-resolution optical measurement system is applied to determine the critical stress intensity factor, as well as to analyse the shape and trajectory of the crack propagation during the test. In the laboratory experiments conducted, the ARAMIS system was applied. ARAMIS is a modular measuring system designed for 2D analyses of statically or dynamically loaded members. It is a part of the ARAMIS family of optical measuring systems developed by Carl Zeiss AG Company, based on digital image correlation technology. The testing is based on high-speed imaging, enabling the accurate study of a crack path during the crack propagation starting from the tip of the initial notch. Before the testing, each beam is covered in a speckle pattern on the side surface in the mid-span of the specimen. The arrangement of the cameras and the test specimen is presented in Fig. 2.

(a) (b)

Fig. 2. The test setup for testing by the ARAMIS system (a); a close-up of the examined area covered by the speckle pattern (b)

During the bend test, the external force signal in cyclic loading is connected to the system. In the next step, the obtained laboratory data is processed by the dedicated Zeiss Inspect software. Surface components and virtual extensometers at the edge of the initial notch are created for each beam.

2.3. The critical stress intensity factor calculations

The critical stress intensity factor, the peak load ($P_{\max}$) and the unloading compliance (C_u) can be determined based on the load-CMOD curve according to the calculation procedure given in RILEM recommendations [20]. The effective crack length (a_c) is calculated based on the unloading compliance. The modulus of elasticity is also necessary for determining K_{Ic} and it can be taken from the laboratory test in accordance with [25].

K_{Ic} is calculated based on the load-CMOD curves from Eq. (2.1):

$$K_{\mathrm{Ic}} = 3(P_{\max} + 0.5W)\frac{S(\pi a_c)^{0.5} \cdot F(\alpha)}{2d^2 b} \tag{2.1}$$

where: $P_{\max}$ – the measured peak load [N], $W = W_o S/L$ [N], W_o – the self-weight of the beam [N], d – the beam depth [mm], b – the beam thickness [mm], S – the loading span [mm],

L – the specimen length [mm], $F(\alpha)$ – the shape function taken from Eq. 2.2:

$$F(\alpha) = \frac{1.99 - \alpha\,(1-\alpha)\,(2.15 - 3.93\alpha + 2.7\alpha^2)}{\sqrt{\pi^{0.5}\,(1+2\alpha)\,(1-\alpha)^{1.5}}} \tag{2.2}$$

where: $\alpha = a_c/d$, a_c – the critical effective crack length [mm] taken from Eq. 2.3:

$$a_c = \frac{6SE_cV_1(\alpha)}{C_u d^2 b} \tag{2.3}$$

where: E_c – the modulus of elasticity of concrete [GPa], C_u – the unloading compliance at 95% of peak load determined from the load-CMOD curve [m · N^{-1}] as presented in Fig. 3, $V_1(\alpha_1)$ – the shape function taken from Eq. 2.4:

$$V_1\,(\alpha_1) = 0.76 - 2.28\alpha_1 + 3.87\alpha_1^2 - 2.04\alpha_1^3 + \frac{0.66}{(1-\alpha_1)^2} \tag{2.4}$$

where: $\alpha_1 = (a_o + H)/(d + H)$, a_o – the initial notch depth [mm], H – the thickness of the clip gauge holder [mm].

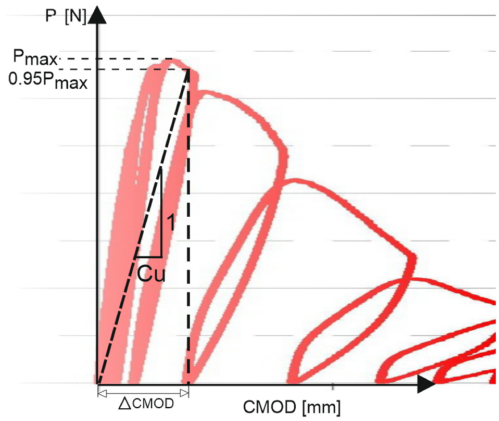

Fig. 3. A graphical method for determining the unloading compliance

3. Experimental investigation

3.1. Test program

The critical stress intensity factor of concrete was tested on beams 700 mm in length and with a cross-sectional dimension of 80 × 150 mm in three-point bend tests using the Materials Test System(MTS), type 809 (MTS Systems Corp.; Eden Prairie, MN, USA). The beams were made with an initial notch of the depth $a_o = 50$ mm. The notch was cut in the middle of the beam span with a diamond saw before testing. The testing configuration and the geometry of the beam specimen were chosen according to RILEM recommendations [20], as it is presented in Fig. 4.

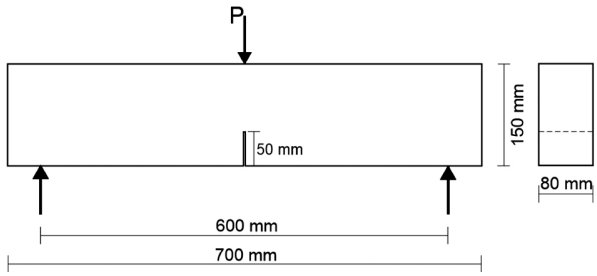

Fig. 4. The setup for the critical stress intensity factor testing

Two types of aggregate were used to make concrete mixtures: gravel aggregate from the Zastawie gravel pit in Poland and dolomite aggregate from the Wszachów quarry in Poland. The maximum aggregate size in concrete mixtures was 16 mm. Two series of samples were distinguished, taking into account the type of aggregate: H16N (concrete with gravel aggregate) and H16D (concrete with dolomite aggregate). Six beams were tested in each series, 3 beams by the standard RILEM method and 3 beams by the method based on the DIC measurements.

Aggregate graining for both types of aggregate was based on similar proportions between the 2.0–8.0 mm and 8.0–16.0 mm fractions (Table 1). When designing the concrete mixtures for both series, the same water-cement ratio (w/c = 0.38) and the same cement (CEM II 42.5R) were used. This ensured the same strength of the hardened cement mortar in both series, which made it possible to analyse the results by taking into account only the characteristics of the aggregate.

Table 1. Composition of concrete mixtures

Series	**Type of aggregate**	**w/c**	**Cement**	**Water**	**Sand 0.0–2.0**	**Coarse aggregate 2.0–16.0**
[–]	**[–]**	**[–]**	**[kg/m^3]**	**[kg/m^3]**	**[kg/m^3]**	**[kg/m^3]**
H16N	gravel	0.38	533.6	205.2	445.5	1204.5
H16D	dolomite	0.38	532.5	204.8	445.5	1204.5

The consistency class of each concrete mixture was determined according to the VeBe method:

– for the H16N series, the time according to VeBe = 13 s, class V2,
– for the H16D series, the time according to VeBe = 12 s, class V2.

Additionally, basic concrete properties were tested, such as the compressive strength, the splitting tensile strength and the modulus of elasticity. Tests of the concrete properties were carried out on standardised cylindrical specimens with a diameter of 150 mm and a height of 300 mm [26]. All tests were carried out after 28 days of curing in water, according to requirements of the Eurocode [27].

3.2. Strength properties of concrete

The compressive strength of concrete was tested in the uniaxial compressive test [28]. For testing the tensile strength of concrete, the Brazilian method was applied, in accordance with [29]. The modulus of elasticity was determined in the uniaxial compressive test according to the rules of "Method A" described in [25]. The obtained concrete properties are presented in Table 2.

Table 2. Concrete properties – test results

Series	Compressive strength			Splitting tensile strength			Modulus of elasticity		
	f_{cm}	σ_s	ν	$f_{ctm,sp}$	σ_s	ν	E_{cm}	σ_s	ν
	[MPa]	[MPa]	[%]	[MPa]	[MPa]	[%]	[GPa]	[GPa]	[%]
H16N	48.1	1.72	3.58	3.54	0.223	6.307	32.5	0.32	0.98
H16D	51.3	1.86	3.63	3.47	0.301	8.673	31.8	1.19	3.74

where:
f_{cm} – mean value of the compressive strength,
$f_{ctm,sp}$ – mean value of the splitting tensile strength,
E_{cm} – mean value of the modulus of elasticity,
σ_s – standard deviation, ν – coefficient of variation.

The compressive strength of concrete with dolomite aggregate (H16D series) was 6.7% higher than the compressive strength of concrete with gravel aggregate (H16N series), whereas the splitting tensile strength and the modulus of elasticity were both approximately 2% lower for concrete in the H16D series, compared to the splitting tensile strength and the modulus of elasticity obtained for concrete in the H16N series. As the differences between the basic properties of the concrete obtained for the two series in the performed experiment were not high, it was concluded that the type of aggregate did not significantly affect the concrete properties. Furthermore, the obtained coefficients of variation for all tested concrete properties exhibited relatively low values, which indicates that the concretes are of good quality.

3.3. Fracture properties of concrete

The load-CMOD curves were obtained from the results of the test performed using the standard RILEM method and based on DIC measurements. All plotted curves had a similar shape consisting of two distinct parts. The initial segment of each load-CMOD curve was characterised by an almost linear relationship, showing a slow, gradual increase in the crack mouth opening displacement. Subsequently, upon reaching the peak load, a more non-linear behaviour became evident, accompanied by observable crack propagation starting at the initial notch tip. Additionally, a noticeable softening phenomenon was observed after the peak load. The reduction in the concrete's ability to resist further cracking was more evident with each subsequent loading cycle, with CMOD increasing more rapidly. These observations agree with fracture mechanics theory for quasi-brittle characteristics of concrete material. The load-CMOD curves plotted from the standard RILEM method are presented in Fig. 5, and the parameters obtained from the three-point bend test are shown in Table 3.

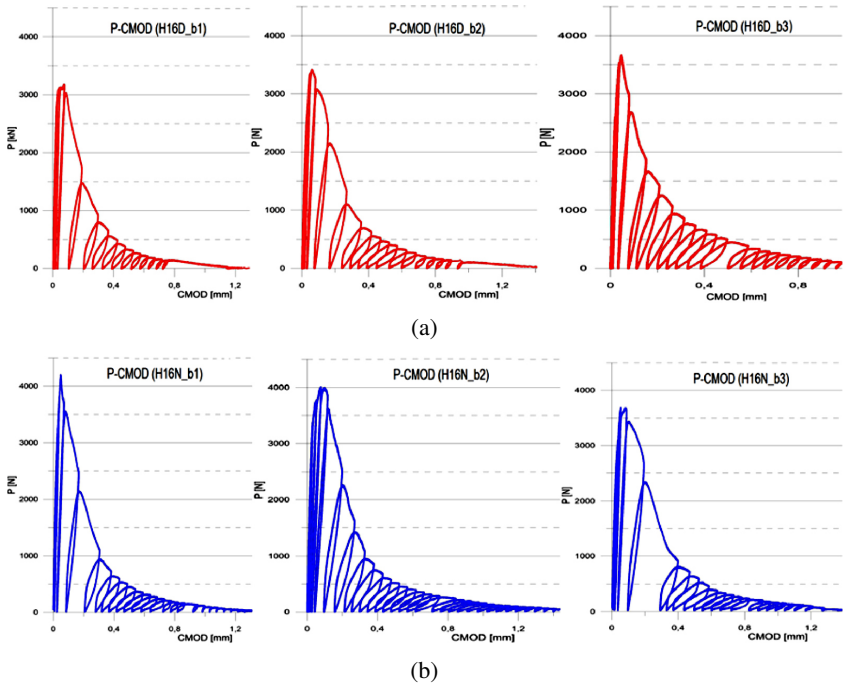

Fig. 5. The load vs crack mouth opening displacement curves plotted manually from the three-point bend test in accordance with RILEM [20]: (a) for the H16D series, (b) for the H16N series

Table 3. Test results based on the load-CMOD curves (RILEM)

Series	The critical stress intensity factor – mean value [MPa$\sqrt{m}$]	The peak load – mean value [N]	CMOD – mean value [mm]
H16D	0.75	3401.0	0.0582
H16N	0.87	3963.1	0.0600

The load-CMOD curves were also obtained based on the virtual measurements from the high-speed imaging from the ARAMIS system (Fig. 6), similar to the RILEM method. The frequency of image recording for each beam was set to 0.3 Hz. The fracture parameters calculated based on the data collected by the ARAMIS system are presented in Table 4.

Table 4. Test results based on the load-CMOD curves (ARAMIS)

Series	The critical stress intensity factor – mean value [MPa$\sqrt{m}$]	The peak load – mean value [N]	CMOD at the peak load – mean value [mm]
H16D	0.71	3352.8	0.0430
H16N	0.84	3910.0	0.0461

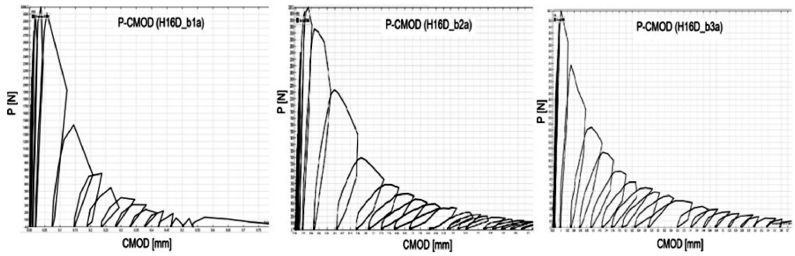

(a)

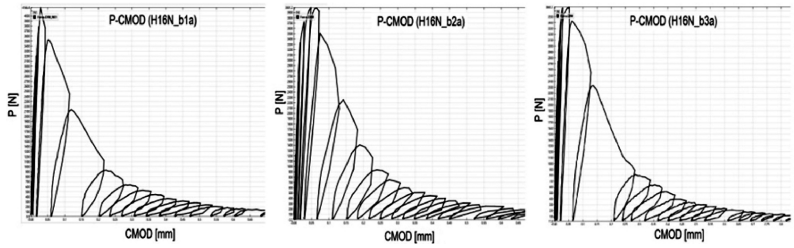

(b)

Fig. 6. The load vs crack mouth opening displacement curves plotted from ARAMIS data: (a) for the H16D series, (b) for the H16N series

4. The analysis of the test results

In the standard RILEM approach, the load-CMOD curves were plotted manually from the raw data obtained from the MTS press, whereas when testing with the use of the DIC-based method, the curves were plotted virtually in the Zeiss Inspect software. Then, on the basis of the obtained curves, the parameters necessary for the critical stress intensity factor were determined: the peak load and the unloading compliance.

Some differences were noted in the results obtained from both methods. The comparison between the critical stress intensity factor, the peak load and the CMOD at peak load derived from the standard RILEM method and based on the ARAMIS measurements is shown in Fig. 7.

The peak load recorded with the DIC technology for the H16D series was 1.4% lower in comparison to the $P_{\max}$ obtained from the standard method. For the H16Nseries, this difference equalled 1.3%. For the series with dolomite aggregate, the critical stress intensity factor was 5.3% lower when calculations were carried out using the load-CMOD curves obtained from the ARAMIS system compared to K_{Ic} derived from the standard method. For the series with gravel aggregate, this difference equalled 3.4%. The highest difference was observed in the case of the CMOD at peak load. For the series with gravel aggregate, the CMOD at the peak load was 23.2% lower for the measurements by the ARAMIS system compared to that derived by the standard RILEM method. In the case of the series with dolomite aggregate, the difference reached 26.1%.

Measurement of all fracture properties $P_{\max}$, CMOD at peak load and K_{Ic} performed by both methods showed the same tendency despite the type of aggregate. Although visible

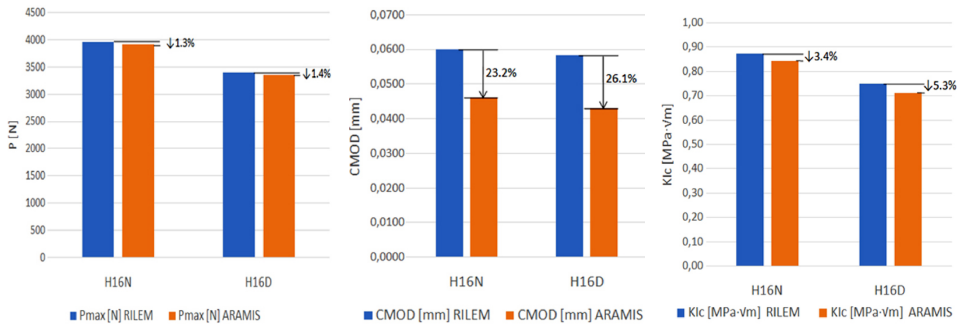

(a) (b) (c)

Fig. 7. The comparison of fracture parameters measured based on the RILEM method and by the ARAMIS system: (a) the peak load $P_{\max}$, (b) crack mouth opening displacement (CMOD) at peak load, (c) the critical stress intensity factor K_{Ic}

differences in CMOD at peak load were measured by both methods, it can be observed that the influence of the testing method on the peak load and the critical stress intensity factor was negligibly small. However, it is also worth noting that $P_{\max}$ and CMOD at peak load are only supporting parameters obtained from the tests. The primary and most significant fracture parameter is K_{Ic}. When determining K_{Ic} not only the geometry of the tested beams is important, but also the concrete modulus of elasticity and the declining shape of the P-CMOD curve. C_u is not directly related to the CMOD obtained at the $P_{\max}$ point, but to the increase in CMOD over the course of the test. The calculation of K_{Ic} based on Eq. 2.2–2.4 takes into account C_u as the inverse slope of the load-CMOD curve at 95% of the peak load (as presented earlier in Fig. 3 above). Thus, the observed differences in CMOD at peak load do not have a significant reflection when determining K_{Ic} as CMOD at peak load is not included in the procedure of the K_{Ic} calculation. It can be concluded that if the basic aim of the investigation is to determine K_{Ic}, both testing methods – the standard RILEM method and DIC-based measurements – give similar results, and they can be used interchangeably.

The comparison of test results presented in Fig. 6 enabled the performance of another step of the analysis, which focused on the influence of the aggregate type on the fracture parameters of concrete. In this stage of the analysis, the results of $P_{\max}$ and K_{Ic} obtained in every series measured by the standard method and using the ARAMIS system were taken together. It was possible to join test results as they were not affected by the type of testing method. The following observations were made for the series with gravel aggregate (H16N) compared to the series with dolomite aggregate (H16D):

– a 14.6% increase in the critical stress intensity factor,
– a 14.2% increase in the peak load.

The fracture parameters for concrete: K_{Ic} and $P_{\max}$ were higher for concrete with gravel aggregate compared to the results for concrete with dolomite aggregate, although the splitting tensile strength and the modulus of elasticity did not depend on the aggregate type.

In order to explain the findings, a deeper analysis of measurements made by the ARAMIS system was done as the ARAMIS system enabled the measurement of deformations on a selected area of the test specimen in the mid-span of each beam. Furthermore, crack propagation could be observed in real time during the laboratory tests and afterwards based on the built surface components in the dedicated computer software.

In the performed experimental investigation, an additional analysis was conducted with regard to data processed in the Zeiss Inspect software. Crack shapes were observed and studied. For the same value of the crack mouth opening displacement, the recorded intensity of strain was higher in the case of the concrete with dolomite aggregate. The examples of crack propagation obtained by the ARAMIS system when CMOD = 0.05 mm for the series with gravel aggregate (H16N) and for the series with dolomite aggregate (H16D) are presented in Fig. 8. The scale for showcasing the strain fields was the same for all specimens in both series. The distinctive non-linear post-peak strain softening started when the CMOD reached 0.05 mm, and therefore, CMOD = 0.05 mm was taken as the comparative level for all tested beam specimens.

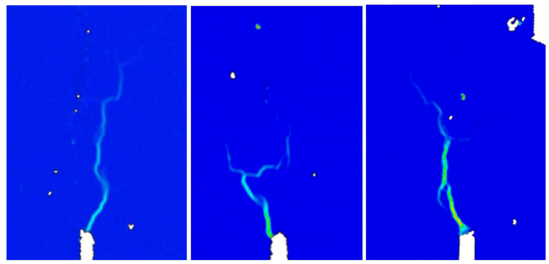

(a)

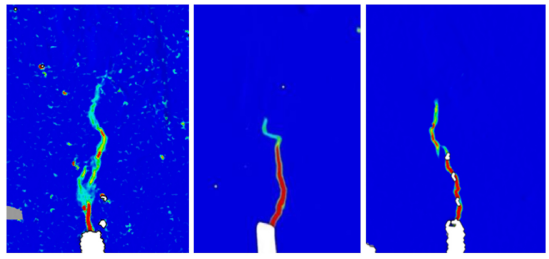

(b)

Fig. 8. Examples of recorded crack propagation paths through the ARAMIS system when CMOD = 0.05 mm: (a) for the series with gravel aggregate (H16N); (b) for the series with dolomite aggregate (H16D). The red colour indicates greater deformation

When examining crack propagation paths resulting from strain fields presented in Fig. 8, a difference was observed in relation to crack development and strain intensity. In some cases, branching and kinking of the main crack appeared, and thus, a more tortuous path of the crack was observed. This indicates that the main crack encountered obstacles, such as the aggregate grains, and changed its trajectory to one requiring less energy for further propagation, as is shown in Fig. 9.

(a) (b)

Fig. 9. Two sides of the fracture surface of the tested beam (from the H16N series) (a) and the corresponding branch of the main crack (b)

It should be noted that the arrangement of aggregate grains within the hardened structure of concrete had an impact on the fracture process and forced the crack to propagate around the inclusions. On the other hand, sometimes, the crack passes through the aggregate grains instead of circumventing them. This phenomenon occurred more often in the concrete with dolomite aggregate (H16D). In the case of concrete with gravel aggregate (H16N), the crack more often surrounded the aggregate grains. On the basis of these observations, the different intensities of crack development can be explained in concrete with dolomite and gravel aggregates.

The images created with the ARAMIS system confirmed that K_{Ic} depended on the aggregate type, and it was lower for concrete with dolomite aggregate than for concrete with gravel aggregate. When examining the strain fields at the same crack mouth opening displacement, a higher intensity of the strain increase was noted for the concrete in the H16D series compared to the concrete in the H16N series. The additional possibilities of data imaging obtained from the ARAMIS application for testing fracture properties of concrete can help in deeper analysis of the processes connected with concrete cracking.

5. Conclusions

Two testing methods for determining the critical stress intensity factor were compared: the standard RILEM method and the DIC-based method. On the basis of the performed research for beam specimens made by concrete with gravel and dolomite aggregates, the following conclusions were drawn:

1. The influence of the testing method on the critical stress intensity factor was negligibly small. Such a conclusion was drawn when testing concrete both with gravel and dolomite aggregates. When determining K_{Ic}, the standard RILEM method and the DIC-based measurements (for example by the ARAMIS system) give comparative results and they can be used interchangeably.

2. The aggregate type had an influence on fracture properties of tested concretes. The critical stress intensity factor, the peak load and the crack mouth opening displacement at peak load were lower in concrete with dolomite aggregate compared to the results obtained in concrete with gravel aggregate.
3. The DIC-based method offered more possibilities for analysing the cracking process in the tested specimens. Through the analysis of the strain maps generated using the ARAMIS system, the differences in K_{Ic} for concrete with different aggregate types can be explained, and the role of aggregate in the process of crack formation can be described.

Summing up, when the only focus of research is to calculate the critical stress intensity factor, it is possible to use both testing methods as they yield comparable results. For a deeper analysis of cracking processes in concrete, the DIC-based measurement technique proves to be a more valuable tool, for example when investigating the role of aggregate type and granulation at cracking processor or analysing the influence of different factors affecting concrete durability on cracking resistance. By examining the accuracy of both the standard RILEM method and the DIC-based method (e.g. the ARAMIS system) when testing fracture properties of concrete, the research paper aims to contribute to the ongoing investigation of the evolution and applicability of concrete testing methodologies.

References

[1] S. Gavela, N. Nikoloutsopoulos, G. Papadakos, D. Passa, and A. Sotiropoulou, "Multifactorial experimental analysis of concrete compressive strength as a function of time and water-to-cement ratio", *Procedia Structural Integrity*, vol. 10, pp. 135–140, 2018, doi: 10.1016/j.prostr.2018.09.020.

[2] A.S. Alemu, J. Yoon, M. Tafesse, Y. Seo, H. Kim, and S. Pyo, "Practical considerations of porosity, strength, and acoustic absorption of structural pervious concrete", *Case Studies in Construction Materials*, vol. 15, 2021, doi: 10.1016/j.cscm.2021.e00764.

[3] G. Srikanth, M. Safiuddin, M.M. Haque, and M. Rizwan, "Study on mechanical properties of concrete using different types of coarse aggregates", *Materials Today: Proceedings,* vol. 65, part 2, pp. 2029–2033, 2022, doi: 10.1016/j.matpr.2022.06.033.

[4] M. Naderi and A. Kaboudan, "Experimental study of the effect of aggregate type on concrete strength and permeability", *Journal of Building Engineering*, vol. 37, 2021, doi: 10.1016/j.jobe.2020.101928.

[5] H. Zhao, L. Zhang, Z. Wu, A. Liu, and M. Imran, "Aggregate effect on the mechanical and fracture behaviours of concrete", *International Journal of Mechanical Sciences*, vol. 243, 2023, doi: 10.1016/j.ijmecsci.2022.108067.

[6] A. Akram and M. Słowik, "The influence of aggregate graining and crushing value on properties of hardened concrete", *Materiały Budowlane*, no. 11, pp. 41–45, 2023, doi: 10.15199/33.2023.11.09 (in Polish).

[7] X. Yao, H. Wang, J. Guan, M. Lu, L. Li, M. Zhang, S. Chen, and J. Xi, "Statistical determination of fracture parameters of concrete with wide variation of water-cement ratio", *Materials Today Communications*, vol. 33, 2022, doi: 10.1016/j.mtcomm.2022.104341.

[8] A. Seitl, A. Benešová, A.P. Pascual, L. Malíková, D. Bujdoš, and V. Bílek, "Fatigue and fracture properties of concrete mixtures with various water to cement ratio and maximum size of aggregates", *Procedia Structural Integrity*, vol. 42, pp. 1512–1519, 2022, doi: 10.1016/j.prostr.2022.12.192.

[9] L. Qing, H. Zhang, and Z. Zhang, "Effect of biochar on compressive strength and fracture performance of concrete", *Journal of Building Engineering*, vol. 78, 2023, doi: 10.1016/j.jobe.2023.107587.

[10] M.R.M. Aliha, A. Razmi, and A. Mousavi, "Fracture study of concrete composites with synthetic fibers additive under modes I and III using ENDB specimen", *Construction and Building Materials*, vol. 190, pp. 612–622, 2018, doi: 10.1016/j.conbuildmat.2018.09.149.

[11] K. Srinivasan, J. Premalatha, and S.A. Srigeethaa, "A performance study on partial replacement of polymer industries waste (PIW) as fine aggregate in concrete", *Archives of Civil Engineering*, vol. 64, no. 3, pp. 45–56, 2018, doi: 10.2478/ace-2018-0028.

[12] A. Starczyk-Kołbyk, "Analysis of the life cycle concrete with the addition of polypropylene fibers", *Archives of Civil Engineering*, vol. 70, no. 2, pp. 23–42, 2024, doi: 10.24425/ace.2024.149849.

[13] T. Zhu, Z. Chen, L. Zhang, G. Nian, Y. Chen, and J. Hao, "Modeling and fracture behavior of mesoscale concrete considering actual aggregate shapes and placement domain shapes", *Construction and Building Materials*, vol. 400, 2023, doi: 10.1016/j.conbuildmat.2023.132821.

[14] X. Wang, H. A. Saifullah, H. Nishikawa, and K. Nakarai, "Effect of water–cement ratio, aggregate type, and curing temperature on the fracture energy of concrete", *Construction and Building Materials*, vol. 259, 2020, doi: 10.1016/j.conbuildmat.2020.119646.

[15] M. Słowik, "The role of aggregate granulation on testing fracture properties of concrete", *Frattura ed Integrità Strutturale*, vol. 15, no. 58, pp. 376–385, 2021.

[16] R. Afshar, L. Faramarzi, M. Mirsayar, and B.J. Ebrahimi, "Aggregate size effects on fracture behavior of concrete SCB specimens", *Construction and Building Materials*, vol. 389, 2023, doi: 10.1016/j.conbuildmat.2023.131628.

[17] M. Rezaei and M.A. Issa, "Specimen and aggregate size effect on the dynamic fracture parameters of concrete under high loading rates", *Engineering Fracture Mechanics*, vol. 260, 2022, doi: 10.1016/j.engfracmech.2021.108184.

[18] M.-H. Zeng, H.-W. Wang, Y.-J. Wang, J.-J. Zheng, and Z.-M. Wu, "Meso-crack propagation process of concrete based on macro-fracture parameters: Numerical and experimental", *Theoretical and Applied Fracture Mechanics*, vol. 129, 2024, doi: 10.1016/j.tafmec.2023.104216.

[19] D. Salauyou and P. Knyziak, „Evaluation of the influence of linear stress concentrators in reinforced concrete elements using the postulates of fracture mechanics", *Acta Scientiarum Polonorum. Architectura*, vol. 22, no. 1, pp. 30–37, 2023, doi: 10.22630/ASPA.2023.22.4.

[20] RILEM TC-89 FMC (Draft Recommendation), "Determination of fracture parameters (K_{Ic} and $CTOD_c$) of plain concrete using three – point bend tests", *Materials and Structures, RILEM Publications SARL*, vol. 23, pp. 457–460, 1990.

[21] G. Golewski, "Measurement of fracture mechanics parameters of concrete containing fly ash thanks to use of Digital Image Correlation (DIC) method", *Measurement*, vol. 135, pp. 96–105, 2019, doi: 10.1016/j.measurement.2018.11.032.

[22] J. Krassowska, M. Kosior-Kazberuk, M. Słowik, and A. Akram, "Sustainable future of construction: the potential of concrete with basalt mini-bars as reinforcement", *Economics and Environment*, vol. 88, no. 1, 2024, doi: 10.34659/eis.2024.88.1.776.

[23] J. Kozicki and J. Tejchman, „Experimental Investigations of Strain Localization in Concrete using Digital Image Correlation (DIC) Technique", *Archives of Hydroengineering and Environmental Mechanics*, vol. 54 no. 1, pp. 3–24, 2007.

[24] B. Turoń, D. Ziaja, L. Būda, and B. Miller, „DIC in Validation of Boundary Conditions of Numerical Model of Reinforced Concrete Beams Under Torsion", *Archives of Civil Engineering*, vol. 64, no. 4, pp. 31–48, 2018, doi: 10.2478/ace-2018-0061.

[25] EN 12390-13:2013 Testing hardened concrete - Part 13: Determination of secant modulus of elasticity in compression. European Committee for Standardization: Brussels, Belgium, 2013.

[26] EN 12390–1:2013–03 Testing Hardened Concrete—Part 1: Shape, Dimensions and Other Requirements for Specimens and Moulds. European Committee for Standardization: Brussels, Belgium, 2013.

[27] EN 12390-2:2019 Testing hardened concrete - Part 2: Making and curing specimens for strength tests. European Committee for Standardization: Brussels, Belgium, 2019.

[28] EN 12390–3:2019–07 Testing Hardened Concrete—Part 3: Compressive Strength of Test Specimen. European Committee for Standardization: Brussels, Belgium, 2019.

[29] EN 12390–6:2011 Testing Hardened Concrete—Part 6: Tensile Splitting Strength of Test Specimen. European Committee for Standardization: Brussels, Belgium, 2011.

Analiza krytycznego współczynnika intensywności naprężeń betonu z kruszywem żwirowym i dolomitowym badanego różnymi metodami

Słowa kluczowe: beton, krytyczny współczynnik intensywności naprężeń, cyfrowa korelacja obrazu, parametry pękania

Streszczenie:

Badania odporności betonu na zarysowanie z punktu widzenia mechaniki pękania polegają na określeniu parametrów pękania, takich jak energia pękania (G_F) czy krytyczny współczynnik intensywności naprężeń (K_{Ic}). K_{Ic} jest jednym z najczęściej stosowanych parametrów do analizy procesów pękania w elementach betonowych, na który mają wpływ między innymi rodzaj kruszywa i maksymalny wymiar ziaren kruszywa. Do wyznaczania K_{Ic} używa się standardowej metody badawczej opartej na teście trójpunktowego zginania zgodnie z normą RILEM TC-89. Nową techniką pomiarową, która daje możliwość określenia krytycznego współczynnika intensywności naprężeń w alternatywny sposób jest cyfrowa korelacja obrazu (DIC). Jednak obie metody pomiarowe podlegają pewnym ograniczeniom, które mogą wpływać na uzyskiwane wyniki. Powstaje zatem pytanie, czy na podstawie pomiarów metodą standardową i metodą opartą na DIC uzyskiwane są porównywalne wyniki parametrów pękania betonu. Badania laboratoryjne opisane w artykule dotyczą wyznaczenia krytycznego współczynnika intensywności naprężeń, zmierzonego dwiema metodami badawczymi: standardową w teście trójpunktowego zginania oraz opartą na pomiarze z użyciem cyfrowej korelacji obrazu. Ponadto przeanalizowano czy rodzaj kruszywa ma znaczenie przy ocenie wpływu metody testowej na wyniki K_{Ic}. W celu określenia krytycznego współczynnika intensywności naprężeń betonu, jako podstawową metodę badawczą zastosowano standardową metodę opisaną w zaleceniach RILEM TC-89, tj. badanie w teście trójpunktowego zginania pod cyklicznym obciążeniem z rejestracją zmian sygnału siły oraz rozwarcia wylotu szczeliny (CMOD). Jako drugą metodę badawczą zastosowano system pomiarowy ARAMIS 2D oparty na cyfrowej korelacji obrazu. Krytyczny współczynnik intensywności naprężeń betonu badano na belkach o długości 700 mm i przekroju poprzecznym 80 × 150 mm z uformowaną szczeliną początkową 50 mm w teście trójpunktowego zginania. Do produkcji mieszanek betonowych wykorzystano dwa rodzaje kruszywa: kruszywo żwirowe oraz kruszywo dolomitowe. Maksymalny wymiar kruszywa w mieszankach betonowych wynosił 16 mm. W każdej serii przebadano sześć belek, 3 belki standardową metodą RILEM i 3 belki metodą opartą na pomiarach DIC. Dla każdej belki opracowano krzywą zależności rozwarcia wylotu szczeliny (CMOD) od siły, na podstawie której określono krytyczny współczynnik intensywności naprężeń, obciążenie maksymalne ($P_{\max}$) i podatność przy odciążaniu (C_u) zgodnie z procedurą obliczeniową podaną w zaleceniach RILEM TC-89. Siła maksymalna zarejestrowane za pomocą technologii DIC dla serii betonów z kruszywem dolomitowym była o 1,4% niższa w porównaniu do tej uzyskanej za pomocą standardowej metody. W przypadku serii betonów z kruszywem żwirowym różnica ta wyniosła 1,3%. Dla serii z kruszywem dolomitowym K_{Ic} było 5,3% niższy, gdy obliczenia przeprowadzono przy użyciu krzywych sił a-CMOD uzyskanych dzięki systemowi ARAMIS w porównaniu do K_{Ic} uzyskanego z metody standardowej. W przypadku serii z kruszywem żwirowym różnica ta wyniosła 3,4%. Największą różnicę zaobserwowano w przypadku rozwarcia wylotu szczeliny przy obciążeniu maksymalnym. W przypadku serii z kruszywem żwirowym CMOD przy obciążeniu maksymalnym było 23,2% niższy w przypadku pomiarów za pomocą systemu ARAMIS w porównaniu do wartości uzyskanej za pomocą standardowej metody RILEM. W przypadku serii z kruszywem dolomitowym różnica wyniosła 26,1%. Jednocześnie zaobserwowano, że parametry pękania betonu: K_{Ic} i $P_{\max}$ były wyższe o około 14%w przypadku betonu z kruszywem żwirowym w porównaniu z wynikami uzyskanymi dla betonu z kruszywem dolomitowym. Na podstawie przeprowadzonych badań

dla próbek belkowych wykonanych z betonu z kruszywem żwirowym i dolomitowym wyciągnięto następujące wnioski: (1) wpływ metody badawczej na krytyczny współczynnik intensywności naprężeń był pomijalnie mały, zarówno w przypadku badań betonu z kruszywem żwirowym, jak i dolomitowym. Podczas określania K_{Ic}, standardowa metoda RILEM i pomiary oparte na DIC za pomocą systemu ARAMIS dają porównywalne wyniki i dla przeprowadzonych badań betonu z kruszywem żwirowym i dolomitowym mogły być stosowane zamiennie, (2) rodzaj kruszywa miał wpływ na parametry pękania badanych betonów. Krytyczny współczynnik intensywności naprężeń, siła maksymalna i krytyczne rozwarcie wylotu szczeliny pierwotnej przy sile maksymalnej były niższe w betonie z kruszywem dolomitowym w porównaniu z wynikami uzyskanymi w betonie z kruszywem żwirowym. Porównanie obu metod badawczych wskazało, że zastosowanie systemu Aramis pozwala na szerszą analizę procesu pękania betonu w badanych próbkach. Na podstawie map odkształceń wygenerowanych za pomocą systemu ARAMIS można przeprowadzić pogłębioną analizę wpływu różnych czynników na proces powstawania rys w betonie i na wartość parametrów pękania betonu, np. K_{Ic}.

Received: 2024-06-04, Revised: 2024-08-15